Author Manuscript

Author Manuscript

Author Manuscript

Author Manuscript

HHS Public Access

Author manuscript

J Mater Sci Mater Med. Author manuscript; available in PMC 2018 October 16.

Published in final edited form as:

J Mater Sci Mater Med. ; 29(5): 54. doi:10.1007/s10856-018-6077-x.

An oxygen plasma treated poly(dimethylsiloxane) bioscaffold coated with polydopamine for stem cell therapy

Mehdi Razavi[1] and **Avnesh S. Thakor**[1]

[1]Department of Radiology, Stanford University, Palo Alto, CA 94304, USA

Abstract

In this study, 3D macroporous bioscaffolds were developed from poly(dimethylsiloxane) (PDMS) which is inert, biocompatible, non-biodegradable, retrievable and easily manufactured at low cost. PDMS bioscaffolds were synthesized using a solvent casting and particulate leaching (SCPL) technique and exhibited a macroporous interconnected architecture with 86 ± 3% porosity and 300 ± 100 μm pore size. As PDMS intrinsically has a hydrophobic surface, mainly due to the existence of methyl groups, its surface was modified by oxygen plasma treatment which, in turn, enabled us to apply a novel polydopamine coating onto the surface of the bioscaffold. The addition of a polydopamine coating to bioscaffolds was confirmed using composition analysis. Characterization of oxygen plasma treated-PDMS bioscaffolds coated with polydopamine (polydopamine coated-PDMS bioscaffolds) showed the presence of hydroxyl and secondary amines on their surface which resulted in a significant decrease in water contact angle when compared to uncoated-PDMS bioscaffolds (35 ± 3%, $P < 0.05$). Seeding adipose tissue-derived mesenchymal stem cells (AD-MSCs) into polydopamine coated-PDMS bioscaffolds resulted in cells demonstrating a 70 ± 6% increase in viability and 40 ± 5% increase in proliferation when compared to AD-MSCs seeded into uncoated-PDMS bioscaffolds ($P < 0.05$). In summary, this two-step method of oxygen plasma treatment followed by polydopamine coating improves the biocompatibility of PDMS bioscaffolds and only requires the use of simple reagents and mild reaction conditions. Hence, our novel polydopamine coated-PDMS bioscaffolds can represent an efficient and low-cost bioscaffold platform to support MSC therapies.

1 Introduction

Regenerative medicine offers the potential to significantly impact a wide spectrum of healthcare issues from diabetes to cardiovascular disease [1]. One area which has attracted significant attention is the development of novel 3D porous bioscaffolds which can accommodate different types of cellular therapy. Bioscaffolds can be created from a plethora of biomaterials which can be specifically chosen based on their (i) intrinsic properties, (ii) ability to integrate into the host tissue and (iii) ability to create an optimal micro-environment to nourish and support cells.

Avnesh S. Thakor, asthakor@stanford.edu.

Compliance with ethical standards

Conflict of interest

The authors declare that they have no conflict of interest.

Author Manuscript Author Manuscript Author Manuscript Author Manuscript

Recently poly(dimethylsiloxane), abbreviated as PDMS (molecular structure 1) [2], has generated considerable attention in numerous biomedical applications including implantable devices, soft tissue implants (i.e. contact lenses), laboratory equipment (i.e., dishes, flasks and well-plates), diagnostic chips (i.e., microarrays for DNA analysis) and microfluidic components [3–8]. PDMS has such a diverse array of application due to its multi-faceted properties which include it being inert, non-toxic, biocompatible, gas permeable, flexible, optically transparent and easily manufactured at low cost [9–13]. These attributes also make it a promising bioscaffold for applications in regenerative medicine.

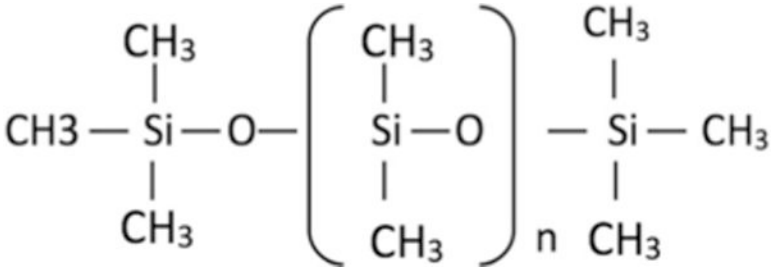

Molecular structure 1

However, the use of unmodified PDMS for cellular therapy is challenging given its intrinsic high surface hydrophobicity due to multiple methyl groups. Indeed, this has been identified as the primary factor for poor cell adhesion on PDMS bioscaffolds with the creation of dissociating islands of cell aggregates. In turn, this renders the surface of PDMS incompatible for cell adhesion and proliferation [14–16].

The surface hydrophilicity of PDMS is often modified when it has to be used for cellular studies [17]. Although different methods have been used to make the surface of PDMS hydrophilic, their implementation have proved to be time-consuming. Moreover, these processes are usually limited by numerous preparation steps and rigorous reaction conditions, which are thereby restrained to a limited number of material categories [18]. For example, one strategy is to coat the surface with extracellular matrix proteins, which has been shown to improve cell adhesion and proliferation. However, cell detachment is typically seen following prolonged culture due to protein dissociation [16, 19]. To overcome this problem, studies have chemically modified the surface of PDMS with (3-aminopropyl)triethoxy silane (APTES) and then used glutaraldehyde to cross-link a protein coating onto the surface of PDMS. Although this surface treatment approach is very effective with improved cell adhesion and proliferation [16, 17], the process is time-consuming with numerous intermediate steps. Moreover, the use of toxic chemicals, such as APTES and glutaraldehyde, poses potential health hazards and creates chemical wastes which are toxic to the environment. Hence, a simple, environmentally safe and effective surface functionalization technique is needed to render the surface of PDMS biocompatible if these bioscaffolds are to be used for cellular therapy. Polydopamine coating has recently become a safe way to satisfy these requirements, especially given that there is no need to use toxic chemicals [20]. Inspired by the composition of adhesive proteins in mussels, thin surface-adherent polydopamine films can be easily formed and strongly adhered onto a wide range of inorganic and organic materials, including noble metals, oxides, polymers,

Author Manuscript Author Manuscript Author Manuscript Author Manuscript

semiconductors, and ceramics [21]. Polydopamine coating is formed through a simple dip-coating of objects for 0.5–2 h in an aqueous solution of dopamine which is an inexpensive material compared to the abovementioned coating materials, thus reducing both the *coating time and procedural cost* [18]. Oxygen plasma treatment has also been extensively used for the surface modification of PDMS devices [22, 23]. During oxygen plasma treatment, polar functional groups include silanol groups (SiOH) are introduced on the surface of PDMS [23]. These groups change the surface properties of PDMS from being hydrophobic to hydrophilic [22], thereby providing a better surface for cells to attach to which is highly desirable for cellular therapy.

The interaction between mesenchymal stem cells and biomaterials has received considerable interest in regenerative medicine [24]. In particular, adipose tissue derived mesenchymal stem cells (AD-MSCs) have been shown to secrete a large spectrum of bioactive molecules which create a unique microenvironment for the regeneration of injured tissues [25]. As AD-MSCs are also immuno-protective and can facilitate cellular survival through the release of trophic factors, several studies are investigating their ability to be co-transplanted with different organs to improve cell engraftment and survival (i.e. the co-transplantation of AD-MSCs and pancreatic islets for the treatment of type 1 diabetes) [26–28].

Hence, in this study the surface of our PDMS bioscaf-folds will be first treated using oxygen plasma treatment and then coated with polydopamine. The latter coating will improve the surface adhesive properties of our bioscaffold as well as reduce any associated *in vivo* toxicity of the bioscaffold following its implantation [29–32]. The structural and physical properties of our polydopamine coated-oxygen plasma treated PDMS bioscaffolds (herein referred to as polydopamine coated-PDMS bioscaffolds) will be evaluated along with their ability to create an environment for the survival and growth of AD-MSCs.

2 Materials and methods

2.1 Bioscaffold synthesis

PDMS bioscaffolds were synthesized using a solvent casting and particulate leaching (SCPL) technique with PDMS (RTV 615 A&B, GE Silicone, USA) as the solvent and sodium chloride (NaCl) crystals (Fisher Scientific, USA) as the particulate. PDMS substrates were prepared by mixing ten parts of the silicone elastomer base (RTV 615 A) with four parts of the curing agent (RTV 615B). Salt particles were sifted through sieves of varying mesh sizes to obtain a specific range of crystal diameters (275–350 μm) before being dried in an oven to remove residual air moisture. We aimed to obtain a 90% porosity in our PDMS bioscaffolds by varying the ratio of PDMS substrate to salt crystal based on the volumetric percentage of salt to the total volume of bioscaffold. The mixture of PDMS substrate and salt particles were then poured and compressed on a microscopic glass slide followed by heat-curing at 130 °C for 24 h to permit cross-linking of the PDMS. The salt particles were then leached by immersing bioscaffolds in deionized water for 72 h on a shaker with a rotational speed of 200 rpm at 37 °C; the water was exchanged twice daily. All bioscaffolds were then washed three times with distilled water to ensure removal of all the chemicals before being sectioned in their wet state. A Kimwipe was then used to wick away any residual water before leaving bioscaffolds to dry at room temperature for 24 h. The

Author Manuscript Author Manuscript Author Manuscript Author Manuscript

bioscaffolds were then sectioned to obtain dimensions of 5 mm length by 5 mm width followed by being dried in an oven at 50 °C for 24 h (Fig. 1a).

2.2 Bioscaffold coating

The surface of synthesized PDMS bioscaffolds were then treated with oxygen plasma using an Oxygen Plasma Cleaner (Gala Prep 5, USA) for 3 min at an oxygen pressure of 0.3 mbar (Fig. 1b). Oxygen plasma treated-PDMS bioscaffolds were then immersed in a dopamine solution (2 mg/ml in 10 mM Tris) at pH 8.5 to self-polymerize the dopa-mine before being placed on a tube rotisserie at 18 rpm for 24 h at 25 °C (Fig. 1b,c). Polydopamine coated-PDMS bioscaffolds (Polydopamine coated-oxygen plasma treated-PDMS bioscaffolds) were then washed three times with distilled water to remove any deposited polydopamine micro-particles and/or excess Tris.

All analyses were then performed on the same size (cubes measuring 5 mm length × 5 mm width × 2 mm thick) and weight (70 mg) of uncoated- and polydopamine coated-PDMS bioscaffolds in their dry state.

2.3 Bioscaffold porosity and density measurement

i. Porosity: The porosity of each bioscaffold was calculated in their dry state using the modified liquid replacement method [11]. Following permeation of bioscaffolds in water for 1 h, the percentage of porosity (P) was determined by calculating the difference between the dry (W_{dry}) and wet (W_{wet}) weights of the bioscaffold according to the equation below (Eq. 1):

$$P = \frac{\left(W_{wet} - W_{dry}\right)/\rho_{water}}{V_{app}} \times 100 \quad (1)$$

where ρ_{water} is the density of water and V_{app} is the apparent volume (cm^3) which was obtained by measuring the dimensions of PDMS bioscaffold. It is assumed that the volume of pores is equal to the volume occupied by the absorbed water, while the amount of water absorbed by the PDMS substrate is negligible.

ii. Density: The volume of each bioscaffold was calculated using the height and diameter of sectioned samples. The volume to weight ratio was then used to obtain each bioscaffold's density (g cm^{-3}) using the equation below (Eq. 2):

$$\rho = \frac{W}{\pi \times \frac{D^2}{4} \times H} \quad (2)$$

where ρ is the apparent density, W is the weight in g, D is the diameter in cm, and H is the thickness of a bioscaffold in cm.

Author Manuscript Author Manuscript Author Manuscript Author Manuscript

Bioscaffold porosity and density measurements were performed on three separate samples from each of the following experimental groups: (1) uncoated and (2) polydopamine coated-PDMS bioscaffolds.

2.4 Bioscaffold structural and chemical analysis

i. Scanning electron microscopy (SEM): Bioscaffolds were dehydrated using 10 min sequential immersions through a standard sequence of 50, 70, 90% and finally 100% absolute ethanol solutions. A Kimwipe was then used to wick away any ethanol solution before allowing bioscaffolds to dry overnight at room temperature to prevent bioscaffolds from cracking during the SEM preparation process. Bioscaffolds were finally coated with Au–Pd using a sputter coater and their morphology was analyzed by a SEM (XL30 Sirion, FEI, USA). SEM was performed on three separate samples from each of the following experimental groups: (1) uncoated and (2) polydopamine coated-PDMS bioscaffolds. At five random locations within each sample, the pore size and wall thickness were measured.

ii. Micro-computed tomography (μ-CT): Bioscaffolds were scanned in a consecutive manner using a high-resolution μ-CT (VivaCT 40, Switzerland) to analyze their 3D architecture and porosity. μ-CT was performed on one sample from each of the following experimental groups: (1) uncoated and (2) polydopa-mine coated-PDMS bioscaffolds.

iii. X-ray photoelectron spectroscopy (XPS): Both qualitative and quantitative information about the presence of different elements on the surface of bioscaffolds were scanned using a VersaProbe 1 Scanning XPS Microprobe with a monochromatic Al K alpha X-ray source (ULVAC-PHI, Physical Electronics, USA) in both survey and high-resolution modes. The survey scan was performed with the pass energy of 117.4 eV, the range of 0–1400 eV, energy step of 1 eV, time/step of 20 ms for three cycles. The high-resolution scan of C1s, N1s and O1s was performed with the pass energy of 23.5 eV, energy step of 0.1 eV and time/step of 50 ms for three cycles. All spectra were collected with the charge neutralization flood gun turned on. Data were processed using the MultiPak program XPS software package. XPS was performed on three separate samples from each of the following experimental groups: (1) uncoated, (2) oxygen plasma treated and (3) polydopamine coated-PDMS bioscaf-folds.

iv. Attenuated total reflection-Fourier transform infrared (ATR-FTIR): Bioscaffolds were scanned over a frequency region of 400–4000 cm^{-1} using an ATRFTIR (Nicolet iS50 FT/IR, USA) spectrometer and the characteristic peaks of infrared transmission spectra recorded. ATR-FTIR was performed on three separate samples from each of the following experimental groups: (1) uncoated, (2) oxygen plasma treated and (3) polydopamine coated-PDMS bioscaffolds.

v. Raman spectroscopy: The Raman spectra of bioscaf-folds were acquired over a Raman shift region of 0–3500 cm^{-1} using a micro-Raman confocal scanning microscope (WiTec 500, USA). Raman spectroscopy was performed on three separate samples from each of the following experimental groups: (1) uncoated, (2) oxygen plasma treated and (3) polydopamine coated-PDMS bioscaffolds.

Author Manuscript Author Manuscript Author Manuscript Author Manuscript

vi. Contact angle: Water contact angles were measured with a Contact Angle Analyzer (Rame-Hart 290, USA) to characterize the wetting properties of the surface of bioscaffolds. A 5 μL drop of de-ionized water was delivered onto the bioscaffold surface by a calibrated syringe. The droplet was then imaged using a video camera to measure the water contact angle. Contact angle analysis was performed on three separate samples from each of the following experimental groups: (1) uncoated, (2) oxygen plasma treated and (3) polydopamine coated-PDMS bioscaffolds.

2.5 Bioscaffold interactions with adipose tissue-derived mesenchymal stem cells (AD-MSCs)

i. AD-MSCs isolation: Mouse adipose tissue was obtained from the lower abdomen in male C57BL6 mice at 6–8 weeks of age. Harvested adipose tissue was then washed with sterile PBS, minced with scissors and then digested with 1 mg/mL type I collagenase (Sigma-Aldrich, USA) in serum-free medium at 37 °C for 3 h. The digestion was then inactivated with an equal volume of Dulbecco's Modified Eagle's medium (DMEM; Gibco, USA) supplemented with 10% fetal bovine serum (FBS; Invitrogen, USA). All samples were then filtered through a 100 μm mesh filter to remove any debris. The cellular pellets were collected and then re-suspended in DMEM-10%FBS-50 U/mL penicillin-50 μg/mL streptomycin in a humidified incubator at 37 °C with 5% carbon dioxide. AD-MSCs from passage number 3–5 were used in our studies.

ii. AD-MSCs Flow Cytometric Characterization: Surface marker expression was analyzed by flow cytometry (Guava® easyCyte system; Millipore, USA) using the Phycoerythrin (PE) conjugated mouse monoclonal antibody against CD105, CD90 and CD34 (Biolegend, USA). Adherent cells were detached by treatment with 0.25%trypsin-EDTA, neutralized with DMEM-10%FBS-50 U/mL penicillin-50 μg/mL streptomycin culture medium and disaggregated into single cells by pipetting. The cells were then incubated with the above antibodies for 40 min at room temperature in the dark, washed twice with PBS, re-suspended with 0.5 mL flow cytometry (FACS) buffer (PBS, 2% FBS, 1%P/S) and then immediately characterized using the Guava® easyCyte system.

iii. AD-MSCs Culture: All assays were carried out on AD-MSCs that were either seeded directly into bioscaffolds (direct contact) or incubated with "bioscaffold medium" (indirect contact). For direct contact, bioscaffolds were sterilized by soaking them in 70% ethanol for 0.5 h after which time they were then rinsed three times in sterilized PBS and placed at the bottom of 96-well plates. AD-MSCs were then seeded into bioscaffolds, achieving a cell density of 5×10^4 cells/well. For indirect contact, AD-MSCs were incubated in complete medium (5×10^4 cells/well) for 24 h to allow attachment. "Bioscaffold medium" was then prepared by incubating a bioscaffold with 2 mL culture medium for 5 days at 37 °C; this medium was then added (50 μl/well) to AD-MSCs which were then left to incubate for a further 10 days.

iv. AD-MSCs Viability and Proliferation: The viability of AD-MSCs was determined using an MTT (4,5-dimethylthiazol-2-yl)-2,5-diphenyltetrazolium bromide assay. Here, 50 μL of MTT solution (0.5 mg/mL) was added to the complete medium in each well and left to

Author Manuscript Author Manuscript Author Manuscript Author Manuscript

incubate at 37 °C for 4 h. Water-soluble MTT is taken up by viable cells and converted to an insoluble formazan. Next, 200 μL of DMSO (to dissolve the formazan) was added to each well and left at 37 °C for a further 10 min before the absorbance was measured at 570 nm using a microplate spectrophotometer system —the absorbance directly relates to the number of viable cells present [33, 34]. Cell viability was determined using the following equation (Eq. 3):

$$Cell\ viability = \frac{OD_{sample}}{OD_{control}} \quad (3)$$

where OD_{sample} is the optical density (absorbance) of AD MSCs (from either direct or indirect contact experiments) and $OD_{control}$ is the optical density (absorbance) of AD MSCs that were not exposed to any bioscaffolds. MTT assay was performed on three separate samples from each of the following experimental groups: (1) control (AD-MSCs that were cultured in culture plates and not exposed to any bioscaffolds), (2) uncoated, and (3) polydopamine coated-PDMS bioscaffolds.

AD-MSCs were labeled using Hoechst 33342 (for cell nuclei; Thermofisher Scientific, USA), fluorescein diacetate (FDA; for live cells, Thermofisher Scientific, USA) and propidium iodide (PI; for dead cells, Thermofisher Scientific, USA) as the Live/Dead staining solution. The culture medium was removed and the Live/Dead staining solution [Hoechst 33342 (50 μL/well), FDA (75 μL/well) and PI (75 μL/well)] was added and incubated with AD-MSCs for 20 min at 37 °C. At the end of the incubation time, the staining solution was removed and cells were washed three times with PBS. The live cell imaging solution (Thermo-fisher Scientific, USA) was then added to each well before imaging. Images were acquired with a Zeiss LSM710 Confocal Microscope at a magnification of ×20 and figures were created with the FIJI software (ImageJ, GNU General Public License). Confocal imaging was performed on three separate samples from each of the following experimental groups: (1) control (AD-MSCs that were cultured in culture plates and not exposed to any bioscaffolds), (2) uncoated, and (3) polydopamine coated-PDMS bioscaffolds. Live/Dead assay was performed on three separate samples from each of the following experimental groups: (1) control (ADMSCs that were cultured in culture plates and not exposed to any bioscaffolds), (2) uncoated, and (3) polydopamine coated-PDMS bioscaffolds.

Cell adhesion was visualized with SEM by acquiring images from 3–5 random locations within each bioscaffold. Sectioned bioscaffolds were washed three times with PBS, fixed using 4% paraformaldehyde for 0.5 h at room temperature and then dehydrated in graded ethanol solutions (50, 70, 90% and finally 100% absolute ethanol). All bioscaffolds were then dried at room temperature, sectioned, sputter coated with Au–Pd and then analyzed with SEM. Cell adhesion was visualized with SEM on three separate samples from each of the following experimental groups: (1) uncoated, and (2) polydopamine coated-PDMS bioscaffolds. SEM images were acquired from five random locations within each sample.

Author Manuscript Author Manuscript Author Manuscript Author Manuscript

To measure the AD-MSCs number, cells were seeded either into the uncoated and polydopamine coated-PDMS bioscaffolds or in a 24-well plate to permit cell attachment. On day 1 and 10, the media was removed and AD-MSCs were rinsed using PBS, lifted with 0.25% trypsin-EDTA solution and then quantified using a hemocytometer. Measurement of AD-MSCs number with a hemocytometer was performed on three separate samples from each of the following experimental groups: (1) control (AD-MSCs that were cultured in culture plates and not exposed to any bioscaffolds), (2) uncoated, and (3) polydopamine coated-PDMS bioscaffolds.

2.6 Statistical analysis

Results were expressed as mean ± standard error of the mean. Statistical analysis of all quantitative data was performed by One-way ANOVA (Analysis of variance) with post-hoc Tukey test (Astatsa.com; Online Web Statistical Calculators, USA) with any differences considered statistically significant when $P < 0.05$.

3 Results

3.1 Bioscaffold porosity and density measurement

Synthesized bioscaffolds measured 60 mm (length) × 20 mm (width) × 2 mm (thickness) correlating to a volume of 3.6 ± 0.35 cm^3, porosity of 86 ± 3% and density of 0.18 ±0.06 mg/mm^3.

3.2 Bioscaffold structural, chemical and physical analysis

Micro (μ)-CT images demonstrated the shape and distribution of pores within the 3D porous structure of bioscaffolds. The pore size and wall thickness were measured as 250 ± 50 μm and 75 ± 25 μm, respectively (Fig. 2a, c, e, g). Uncoated-PDMS bioscaffolds were white in color and retained a 3D architecture throughout their processing. Following the immersion of bioscaffolds into a polydopamine solution, a thin adherent polymer layer of dopa-mine was noted which changed the color of each bioscaffold from white to brown (Fig. 2b, d, f, h).

Using XPS, both types of bioscaffold (i.e., uncoated and polydopamine coated) showed peaks corresponding to elements of silicon (Si), carbon (C), nitrogen (N) and oxygen (O). A high-resolution scan of the C1s, O1s and Si2p binding energy depicted the photoemission peaks appearing at 288.5, 536.5 and 106.5 eV, respectively. The C1s, O1s, Si2s and Si2p peaks correspond to the molecular formula of PDMS and the detection of a N1s peak from polydopamine coated-PDMS bioscaffold confirming the existence of amine groups within the polydopamine coating layer. Coating bioscaffolds with polydopamine also changed their surface chemical composition resulting in an increase in C and O and a decrease in Si content. The XPS spectra of the PDMS bioscaffold exhibited an O1s/C1s ratio of 1.3, 1.65 and 1.25 for the uncoated, oxygen plasma treated and polydopamine coated-PDMS bioscaffold, respectively (Fig. 3a, b).

The ATR-FTIR spectra of PDMS bioscaffolds indicated a doublet at 1100 and 1020 cm^{-1} that corresponds to asymmetric (υ_{ass}) and symmetric (υ_s) stretching vibrations of the two

Author Manuscript Author Manuscript Author Manuscript Author Manuscript

neighbor siloxane bonds, respectively. The absorptions at 1259 and 800 cm^{-1} are assigned to the in-plane bending or scissoring and out-of-plane oscillations of the $Si–CH_3$ bonding, respectively. A spectral change was noticeable with an absorption peak at 1722 cm^{-1} and a broad peak in 3100–3600 cm^{-1} upon oxygen plasma treatment related to C = O and –OH functional groups, respectively. An increase in the oxygen-containing peaks also revealed the oxygen insertion into the matrix of PDMS bioscaffold by the oxygen plasma treatment. In the spectrum of polydopamine coated-PDMS bioscaffold, the peaks in the range of 1500–1600 cm^{-1} are assigned to the N−H vibrations and the broad peak spanning 3200–3500 cm^{-1} corresponds to the hydroxyl structures as well as water. The expected signal from carbonyl group (C = O) was also observed at 1700 cm^{-1} (Fig. 3c).

Raman spectroscopy demonstrated methyl group stretching vibrations at 2965 and 2907 cm^{-1}, methyl bending vibrations at 1412 and 1262 cm^{-1}, $Si–CH_3$ rocking vibrations at 862, 787 and 687 cm^{-1} and Si–O–Si stretching vibrations at 488 cm^{-1}. Two broad peaks also appeared at ~1370 and 1630 cm^{-1} corresponding to vibrations of catechol moieties following polydopamine coating of our bioscaffolds (Fig. 3d).

Contact angle analysis showed that uncoated PDMS-bioscaffolds exhibited a high contact angle of 110.5 ± 3°; however, surface treatments significantly decreased the hydrophobicity of bioscaffolds resulting in a decrease in contact angle to 84.2 ± 4° and 54.7 ± 4° following the oxygen plasma treatment and polydopamine coating, respectively ($P < 0.05$, Fig. 3e, f).

3.3 Bioscaffold interactions with adipose tissue-derived mesenchymal stem cells (AD-MSCs)

AD-MSCs expressed CD105 and CD90 surface antigen markers (positive, Fig. 4a, b) with no expression of the CD34 marker (negative, Fig. 4c). Relative to the control group (AD-MSCs cultured in traditional cell culture plates), there was a significantly greater viability of AD-MSCs when they were seeded into bioscaffolds. The results of MTT (Fig. 5a, c) and Live/Dead assays (Fig. 5b, d) from both direct (Fig. 5a, b) and indirect (Fig. 5c, d) cell culture methods at day 10 indicated that AD-MSCs seeded into the polydopamine coated-PDMS bioscaffolds had a higher viability compared to uncoated-PDMS bioscaffolds and the control group. For example, from the results of the MTT assay at day 10, AD-MSCs seeded into uncoated-PDMS bioscaffolds demonstrated a 0.76 ± 0.36-fold increase in cell viability compared to the control group. The addition of a polydopamine coating to bioscaffolds resulted in a 70 ± 6% increase in cell viability (2.55 ± 0.16 vs. 0.76 ± 0.36; Fig. 5a, $P < 0.05$) with the Live/Dead assay also demonstrating an increase in the percentage of live AD-MSCs from 85 ± 4% to 96 ± 4% (Fig. 5b, $P < 0.05$).

Confocal images showed that AD-MSCs seeded into bioscaffolds were higher in number (Fig. 6b, c, e, f, h, i) compared to AD-MSCs cultured alone in traditional cell culture plates (control group; Figure 9a,d,g, $P < 0.05$). These results suggest that AD-MSCs were able to proliferate into bioscaffolds, with a significantly higher degree of proliferation demonstrated in polydopamine coated-PDMS bioscaffolds (Fig. 6c, f) at day 1 (Fig. 6c) and day 10 (Fig. 6f) compared to AD-MSCs cultured in uncoated-PDMS bioscaffolds (Fig. 6b, e, $P < 0.05$). Moreover, ADMSCs were distributed evenly throughout the pores of the bioscaffolds (Fig. 6b, c, e, f; white arrows). SEM images showed the morphology of seeded AD-MSCs within

Author Manuscript Author Manuscript Author Manuscript Author Manuscript

all PDMS bioscaffolds as having a long and thin morphology with widely dispersed filopodia and flattened polygonal extensions (Fig. 6j–m).

AD-MSCs counting using a hemocytometer at day 1 and 10 showed that AD-MSCs seeded into bioscaffolds resulted in a higher proliferation compared to cells cultured alone in a traditional cell culture plate (control group). However, AD-MSCs proliferated more when seeded into polydopamine coated-PDMS bioscaffolds when compared to AD-MSCs seeded into uncoated-PDMS bioscaffolds (Fig. 6n, $P < 0.05$). For example, at day 1, AD-MSCs with same number (50,000) were seeded in each group and at day 10, the number of AD-MSCs seeded into polydopamine coated-PDMS bioscaffolds showed a 40 ± 5% increase when compared to uncoated-PDMS bioscaffolds (500,000 ± 70,000 vs. 300,000 ± 50,000, $P < 0.05$) which was significantly higher than the control group (i.e., 270,000 ± 30,000, $P < 0.05$). Together, these results suggested that AD-MSCs were capable of proliferating more in bioscaf-folds, and especially in polydopamine coated-PDMS bioscaffolds, when compared to the control group.

4 Discussion

PDMS is a polymer that has been utilized for numerous biomaterial and tissue engineering applications. The salient characteristics of PDMS include its tunable elastomeric properties, low cost, gas permeability, optical transparency, low auto-fluorescence, nano-scale precision and easy moldability [17, 35–37]. Hence, PDMS provides a suitable “base-biomaterial” for the fabrication of porous 3D bioscaffolds. Studies have shown that the pore size of 3D bioscaffolds is crucial for determining their function—small pores provide better nutrient and oxygen transfer to facilitate cell growth and proliferation and large pores (i.e., ≥ 300 μm) provide a high surface area to accommodate cells while also facilitating their viability and rate of proliferation [38, 39]. Structural analysis of our PDMS bioscaffold demonstrated it to have a mean pore size of 300 ± 100 μm with a corresponding increase in AD-MSC viability and proliferation compared to AD-MSCs cultured on conventional 2D culture plates. Our bioscaffold also has a high degree of porosity (86 ± 3%) and interconnected macro-pores which creates a physical space to facilitate cell movement and distribution throughout the bioscaffold. In turn, this helps with nutrient and oxygen transfer to cells seeded into the bioscaffold, preventing cell loss from cellular overcrowding as well as providing a substrate for cells to adhere to, and proliferate on, while also interacting with their surrounding environment in all three dimensions [40, 41]. In addition, our results show that our bioscaffolds are soft, compliable and elastic since they can be compressed to a fraction of their original volume before returning to their original shape—properties which have also been shown to promote cell proliferation [42].

Many surface coating strategies have been reported for modifying the hydrophobic surface of PDMS [43–45]. One promising technique is oxygen plasma treatment which has been shown to enhance the hydrophilicity of PDMS bioscaffolds by introducing polar functional groups, especially the silanol group (SiOH), at the expense of methyl groups [46, 47]. This is supported by our data which shows a significant decrease in contact angle from 110.5 ± 3° to 84.2 ± 4° indicating a significant decrease in surface hydrophobicity following oxygen plasma treatment. Plasma is commonly employed because treatments are fast (in the order of

Author Manuscript Author Manuscript Author Manuscript Author Manuscript

minutes) and the chemical modifications are consistent and reproducible. In addition, no special chemicals or waste removal are needed since gaseous byproducts are removed under vacuum. The generation of high energy oxygen species (including electrons, ions, and radicals) within the oxygen plasma will oxidize the organic species on the surface of PDMS bioscaffolds to form H_2O, CO, CO_2 and lower molecular weight hydrocarbons [22, 48]. The spectral change in our ATR-FTIR spectra in our bioscaffold after oxygen plasma treatment was noticeable with two absorption peaks at 1722 cm^{-1} and a broad noticeable absorption peak at 3100–3600 cm^{-1}; these represent the presence of C=O and –OH groups within the surface of our bioscaffold following oxygen plasma treatment [46, 47].

Oxygen plasma treated surfaces do however undergo hydrophobic recovery within minutes [49], mainly due to reorientation of polar groups on the treated surface [50], diffusion of pre-existing low-molecular-weight species from the substrate to the treated surface [12] and condensation of hydroxyl groups [51]. The recovery time is also affected by the conditions in which PDMS bioscaffolds are stored in which include temperature [52], humidity [53] and the presence of aqueous fluid [54] and surfactants [55]. Previous research has shown that storing oxygen plasma treated-PDMS devices in de-ionized water enables them to maintain their hydrophilicity for weeks [22]. Hence, we stored our PDMS bioscaffolds in de-ionized water immediately after oxygen plasma treatment. As oxygen plasma treatment makes the PDMS surface rough [22] and brittle [56], it has the advantage of increasing the bonding strength between a coating layer and the underling PDMS bioscaf-fold [57]. Furthermore, the addition of another layer on top of the oxygen plasma treated PDMS surface has also been shown to prevent its hydrophobic recovery by mechanically stabilizing the surface [56]. Hence, we coated our oxygen plasma treated-PDMS bioscaffolds with polydopamine.

PDMS is a widely-used biomaterial for the investigation of cell substrate interactions and biochip fabrication [58]. Regardless of the application of PDMS, the intrinsic PDMS surface hydrophobicity usually inhibits cell adhesion on the PDMS surface, and PDMS surface modification is required for effective cell adhesion [58]. Many surface coating strategies have been previously reported for the improvement of cell function on PDMS substrates [17, 58–60]. For example, Gomathi and colleagues [60] showed that oxygen plasma treatment on PDMS could enhance adhesion and viability of 3T3 fibroblast cells. However, polydopamine coating has aroused great interest as a new route to the coating of biomaterials, due to its simplicity and material independency in deposition, favorable interactions with cells, and strong reactivity for secondary functionalization [61]. Dopamine undergoes oxidative polymerization in alkaline conditions and has a strong adsorption onto a wide variety of substrates through covalent bonding and strong intermolecular interactions from its repeating 3,4-dihydroxy-L-phenylalanine-lysine (DOPA-K) motif [21, 29, 62]. Interestingly, polydopamine has been shown to reduce the *in vivo* toxicity of bioscaffolds and has been shown to improve cell behavior on various substrates [43–45, 63]. For these reasons, we coated our PDMS bioscaffold with polydopamine which resulted in a further significant decrease in the water contact angle of our bioscaffolds. In addition, the surface chemistry profile of our bioscaffolds demonstrated C = O and –OH functional groups and N1s peak following oxygen plasma treatment and polydopamine coating [59]. Together, this translated to an increase in ADMSC viability and proliferation in the polydopamine coated PDMS

Author Manuscript Author Manuscript Author Manuscript Author Manuscript

bioscaffolds. Polydopamine coating has also been shown to increase the surface adhesive properties of bioscaffolds by acting as a strong anchor between cells and substrates [21, 30–32]. The free amine groups of polydopamine has been shown to enhance cell adhesion and growth given that they confer hydrophilicity and positive charge to substrates [64, 65]. These attributes will therefore enable cells to spread and grow more efficiently in polydopamine coated-PDMS bioscaffolds [17], which was evident in our study with a higher number of AD-MSCs remaining on polydopamine coated bioscaffolds after 10 days when compared to the uncoated bioscaffolds and traditional cell culture plates.

In our study we used a double layer coating (i.e., oxygen plasma treatment and polydopamine coating) as a novel surface modification technique for PDMS-based bioscaffolds. The adhesion of fibroblasts and megakaryocytes (bone marrow cells) to polydopamine coated surfaces has been previously highlighted by Lee and colleagues [21]. Fibroblast cell adhesion was supported on polydopamine coated surface as well as on unmodified controls, while limited megakaryocytic adhesion was observed on polydopamine coated surfaces. These observations indicate that the cytocompatibility of polydopamine coated surfaces appear to be cell type-dependent. In our study we used AD-MSCs and our results demonstrated an increase in AD-MSCs viability and proliferation in the polydopamine coated oxygen plasma treated-PDMS bioscaffolds compared to uncoated PDMS bioscaffolds. This improvement in AD-MSCs function can be due to the polydopamine coating resulting in better biocompatibility and improved surface wett-ability compared to uncoated PDMS. Chuah and colleagues [17] have also reported that the surface of PDMS changes following polydopamine coating as demonstrated by changes in surface wettability as well as the addition of hydroxyl and secondary amines. Our results support this, with data also showing a reduction in the contact angle of PDMS following polydopamine coating which we believe contributes to the improved adhesion and proliferation of AD-MSCs within our polydopamine coated PDMS bioscaffolds. Similar beneficial effects of polydopamine on MSCs have also been reported by Rim and colleagues who analyzed the effect of polydopamine coated-poly(L-lactide) electrospun fibers on human MSCs (hMSCs). These studies concluded that the relative viability of cells cultured on polydopamine coated-fibers was double that of the uncoated fibers and that the coated fibers also supported the proliferation of hMSCs [59].

PDMS has been extensively exploited to study stem cell physiology in the field of mechanobiology and microfluidic chips due to their transparency, low cost and ease of fabrication [17]. However, the use of PDMS as a bioscaffold for regenerative medicine has been less investigated. In this study we developed a PDMS bioscaffold; however, the intrinsic high hydrophobicity of PDMS rendered its surface incompatible for prolonged cell adhesion and proliferation. We therefore introduced a simple coating technology (i.e., oxygen plasma treatment and polydopamine coating) which significantly enhanced the biocompatibility of our PDMS bioscaffolds. Our modified PDMS bioscaffold can now be used as a platform for MSC based therapies within regenerative medicine studies. Moreover, this coating technology can be applied to other PDMS-based biomaterials for mechanobiology and microfluidic chips applications.

Author Manuscript Author Manuscript Author Manuscript Author Manuscript

Future studies using our bioscaffold will investigate the beneficial effect of our 3D bioscaffold with other cells lines including human MSCs. Given the highly reactive amine groups in polydopamine, we will also investigate secondary conjugation reactions with various functional groups, including vascular endothelial growth factor (VEGF). Previous studies have also shown that VEGF can be immobilized on the surface of polydopamine using relatively simple techniques [66], which, in turn, demonstrates the robustness of polydopamine as an intermediate layer for the attachment of growth factors. Hence, our next series of experiments will explore the addition of VEGF onto our polydopamine coated-PDMS bioscaffolds; we hypothesize that this will help promote angiogenesis and blood vessel growth into our bioscaffold thereby opening up possibilities for the engraftment of our bioscaffold into living subjects.

5 Conclusion

PDMS bioscaffolds with 86 ± 3% porosity and 300 ± 100 μm pore size were synthesized using a SCPL technique and coated with polydopamine. The results from the present study demonstrate that coating the macroporous PDMS bioscaffolds with polydopamine decreases their water contact angle (35 ± 3%), when compared to uncoated-PDMS bioscaffolds. Seeding AD-MSCs into polydopamine coated-PDMS bioscaffolds increased their viability (70 ± 6%) and proliferation (40 ± 5%) when compared to AD-MSCs seeded into uncoated-PDMS bioscaffolds. In summary, our results show the potential for polydopamine coated-PDMS bioscaffolds in regenerative medicine as an efficient, low-cost matrix which can protect and support AD-MSCs.

Acknowledgements

This work was supported by Stanford Nano Shared Facilities (SNSF) grant (1161726–146-DAARZ), as part of the grant supported by the National Science Foundation grant (ECCS-1542152) and the Stanford Neuroscience Microscopy Service grant (NIH NS069375).

References

1. Nolan K, Millet Y, Ricordi C, Stabler CL. Tissue engineering and biomaterials in regenerative medicine. Cell Transplant. 2008;17:241–243. [PubMed: 18522227]
2. Danilov V, Dölle C, Ott M, Wagner H, Meichsner J. Plasma treatment of polydimethylsiloxane thin films studied by infrared reflection absorption spectroscopy. 29thICPIG, July 12–17, Cancún, México, https://pdfs.semanticscholar.org/dafa/f2d21dde70ccda35056a4f0113ae4aaaadda.pdf?_ga=2.94902553.463489516.1524765127-1439881367.1524765127. 2009.
3. Matsuda K, Suzuki S, Isshiki N, Ikada Y. Re-freeze dried bilayer artificial skin. Biomaterials. 1993;14:1030–5. [PubMed: 8286670]
4. Kiremitçi M, Şerbetçi AI, Çolak R, Pişkin E. Cell attachment to PU and PHEMA based biomaterials: relation to structural properties. Clin Mater. 1991;8:9–16.
5. Khorasani MT, Mirzadeh H. BHK cells behaviour on laser treated polydimethylsiloxane surface. Colloids Surf B Biointerfaces. 2004;35:67–71. [PubMed: 15261058]
6. Liu M, Chen Q. Characterization study of bonded and unbonded polydimethylsiloxane aimed for bio-micro-electromechanical systems-related applications. J Micro/Nanolithogr, MEMS, Moems. 2007;6:23008.
7. Khanafer K, Duprey A, Schlicht M, Berguer R. Effects of strain rate, mixing ratio, and stress-strain definition on the mechanical behavior of the polydimethylsiloxane (PDMS) material as related to its biological applications. Biomed Micro. 2009;11:503–8.

Author Manuscript Author Manuscript Author Manuscript Author Manuscript

8. Colas A, Curtis J. Silicone biomaterials: history and chemistry & medical applications of silicones. Repr Biomater Sci. 2005;80–6:697–707.
9. Pedraza E, Brady AC, Fraker CA, Stabler CL. Synthesis of macroporous poly(dimethylsiloxane) scaffolds for tissue engineering applications. J Biomater Sci Ed. 2013;24:1041–56.
10. Hassler C, Boretius T, Stieglitz T. Polymers for neural implants. J Polym Sci Part B Polym Phys2011;49:18–33.
11. Si J,Cui Z,Xie P,Song L,Wang Q,Liu Q, et al. Characterization of 3D elastic porous polydimethylsiloxane (PDMS) cell scaffolds fabricated by VARTM and particle leaching. J Appl Polym Sci. 2016;42909:1–9.
12. Bodas D, Khan-Malek C. Hydrophilization and hydrophobic recovery of PDMS by oxygen plasma and chemical treatment-An SEM investigation. Sens Actuators, B Chem. 2007;123:368–73.
13. Halldorsson S, Lucumi E, Gómez-Sjöberg R, Fleming RMT. Advantages and challenges of microfluidic cell culture in polydimethylsiloxane devices. Biosens Bioelectron. 2015;63:218–31. [PubMed: 25105943]
14. Lee JN, Jiang X, Ryan D, Whitesides GM. Compatibility of mammalian cells on surfaces of poly(dimethylsiloxane). Langmuir. 2004;20:11684–91. [PubMed: 15595798]
15. Fuard D, Tzvetkova-Chevolleau T, Decossas S, Tracqui P, Schiavone P. Optimization of poly-di-methyl-siloxane (PDMS) substrates for studying cellular adhesion and motility. Microelectron Eng. 2008;85:1289–93.
16. Chuah YJ, Kuddannaya S, Lee MHA, Zhang Y, Kang Y. The effects of poly(dimethylsiloxane) surface silanization on the mesenchymal stem cell fate. Biomater Sci. 2015;3:383–90. [PubMed: 26218129]
17. Chuah YJ, Koh YT, Lim K, Menon NV, Wu Y, Kang Y. Simple surface engineering of polydimethylsiloxane with polydopamine for stabilized mesenchymal stem cell adhesion and multipotency. Sci Rep. 2015;5:18162. [PubMed: 26647719]
18. Ye Q, Zhou F, Liu W. Bioinspired catecholic chemistry for surface modification. Chem Soc Rev. 2011;40:4244. [PubMed: 21603689]
19. Kuddannaya S, Chuah Y. Surface chemical modification of poly (dimethylsiloxane) for the enhanced adhesion and proliferation of mesenchymal stem cells. ACS Appl Mater Interfaces. 2013;5:9777–84. [PubMed: 24015724]
20. Huang S, Liang N, Hu Y, Zhou X, Abidi N. Polydopamine-assisted surface modification for bone biosubstitutes. Biomed Res. Int 2016;2016:1–9.
21. Lee H, Dellatore SM, Miller WM, Messersmith PB. Mussel-inspired surface chemistry for multifunctional coatings. Science. 2007;318:426–30. [PubMed: 17947576]
22. Tan SH, Nguyen NT, Chua YC, Kang TG. Oxygen plasma treatment for reducing hydrophobicity of a sealed polydimethylsiloxane microchannel. Biomicrofluidics. 2010;4:32204. [PubMed: 21045926]
23. Hillborg H, Ankner JF, Gedde UW, Smith GD, Yasuda HK, Wikström K. Crosslinked polydimethylsiloxane exposed to oxygen plasma studied by neutron reflectometry and other surface specific techniques. Polymer (Guildf). 2000;41:6851–63.
24. Bhat S, Kumar A. Biomaterials in regenerative medicine. J Post Med Edu Res. 2012;46:81–9.
25. Caplan AI. Adult mesenchymal stem cells for tissue engineering versus regenerative medicine. J Cell Physiol. 2007;213:341–7. [PubMed: 17620285]
26. Serup P, Madsen OD, Mandrup-Poulsen T. Islet and stem cell transplantation for treating diabetes. BMJ. 2001;322:29–32. [PubMed: 11141151]
27. Krishnan R, Alexander M, Robles L, Foster CE, Lakey JRT. Islet and stem cell encapsulation for clinical transplantation. Rev Diabet Stud. 2014;11:84–101. [PubMed: 25148368]
28. Ito T, Itakura S, Todorov I, Rawson J, Asari S, Shintaku J, et al. Mesenchymal stem cell and islet co-transplantation promotes graft revascularization and function. Transplantation. 2010;89: 1438–45. [PubMed: 20568673]
29. Yang F, Zhao B. Adhesion properties of self-polymerized dopa-mine thin film. Open Surf Sci J. 2011;3:115–22.

Author Manuscript Author Manuscript Author Manuscript Author Manuscript

30. Tsai WB, Chen WT, Chien HW, Kuo WH, Wang MJ. Poly (dopamine) coating of scaffolds for articular cartilage tissue engineering. Acta Biomater. 2011;7:4187–94. [PubMed: 21839186]
31. Ko E, Yang K, Shin J, Cho SW. Polydopamine-assisted osteoinductive peptide immobilization of polymer scaffolds for enhanced bone regeneration by human adipose-derived stem cells. Biomacromolecules. 2013;14:3202–13. [PubMed: 23941596]
32. Tsai WB, Chen WT, Chien HW, Kuo WH, Wang MJ. Poly (dopamine) coating to biodegradable polymers for bone tissue engineering. J Biomater Appl. 2014;28:837–48. [PubMed: 24381201]
33. Pariente J-L, Kim B-S, Atala A. In vitro biocompatibility evaluation of naturally derived and synthetic biomaterials using normal human bladder smooth muscle cells. J Urol. 2002;167:1867–71. [PubMed: 11912450]
34. Song E, Yeon Kim S, Chun T, Byun HJ, Lee YM. Collagen scaffolds derived from a marine source and their biocompatibility. Biomaterials. 2006;27:2951–61. [PubMed: 16457878]
35. Duffy DC, McDonald JC, Schueller OJA, Whitesides GM. Rapid prototyping of microfluidic systems in poly(dimethylsiloxane). Anal Chem. 1998;70:4974–84. [PubMed: 21644679]
36. McDonald JC, Whitesides GM. Poly(dimethylsiloxane) as a material for fabricating microfluidic devices. Acc Chem Res. 2002;35:491–9. [PubMed: 12118988]
37. Mata A, Fleischman AJ, Roy S. Characterization of polydimethylsiloxane (PDMS) properties for biomedical micro/nano-systems. Biomed Micro. 2005;7:281–93.
38. Kumari J, Karande AA, Kumar A. Combined effect of cryogel matrix and temperature-reversible soluble-insoluble polymer for the development of in vitro human liver tissue. ACS Appl Mater Interfaces. 2016;8:264–77. [PubMed: 26654271]
39. Matsiko A, Gleeson JP, O'Brien FJ. Scaffold mean pore size influences mesenchymal stem cell chondrogenic differentiation and matrix deposition. Tissue Eng Part A. 2015;21:486–97. [PubMed: 25203687]
40. Bencherif SA, Warren Sands R, Ali OA, Li WA, Lewin SA, Braschler TM, et al. Injectable cryogel-based whole-cell cancer vaccines. Nat Commun. 2015;6:7556. [PubMed: 26265369]
41. Mandal BB, Kundu SC. Cell proliferation and migration in silk fibroin 3D scaffolds. Biomaterials. 2009;30:2956–65. [PubMed: 19249094]
42. Kumari J,Kumar A, Development of polymer based cryogel matrix for transportation and storage of mammalian cells. Sci Rep [Internet]. 2017;7:41551.
43. Yoo HS, Kim TG, Park TG. Surface-functionalized electrospun nanofibers for tissue engineering and drug delivery. Adv Drug Deliv Rev. 2009;61:1033–42. [PubMed: 19643152]
44. Martins A, Pinho ED, Faria S, Pashkuleva I, Marques AP, Reis RL, et al. Surface modification of electrospun polycaprolactone nanofiber meshes by plasma treatment to enhance biological performance. Small. 2009;5:1195–206. [PubMed: 19242938]
45. Ma Z, Gao C, Gong Y, Shen J. Cartilage tissue engineering PLLA scaffold with surface immobilized collagen and basic fibroblast growth factor. Biomaterials. 2005;26:1253–9. [PubMed: 15475055]
46. Yu H, Chong ZZ, Tor SB, Liu E, Loh NH. Low temperature and deformation-free bonding of PMMA microfluidic devices with stable hydrophilicity via oxygen plasma treatment and PVA coating. RSC Adv. 2015;5:8377–88.
47. Hui AYN, Wang G, Lin B, Chan W-T. Microwave plasma treatment of polymer surface for irreversible sealing of micro-fluidic devices. Lab Chip. 2005;5:1173–7. [PubMed: 16175276]
48. Tsougeni K, Vourdas N, Tserepi A, Gogolides E, Cardinaud C. Mechanisms of oxygen plasma nanotexturing of organic polymer surfaces: from stable super hydrophilic to super hydrophobic surfaces. Langmuir. 2009;25:11748–59. [PubMed: 19788226]
49. Bhattacharya S, Datta A, Berg JM, Gangopadhyay S. Studies on surface wettability of poly(dimethyl) siloxane (PDMS) and glass under oxygen-plasma treatment and correlation with bond strength. J Micro Syst. 2005;14:590–7.
50. Morra M, Occhiello E, Marola R, Garbassi F, Humphrey P, Johnson D. On the aging of oxygen plasma-treated polydimethylsiloxane surfaces. J Colloid Interface Sci. 1990;137:11–24.
51. Tóth A, Bertóti I, Blazsó M, Bánhegyi G, Bognar A, Szaplonczay P. Oxidative damage and recovery of silicone rubber surfaces. I. X-ray photoelectron spectroscopic study. J Appl Polym Sci. 1994;52:1293–307.

Author Manuscript Author Manuscript Author Manuscript Author Manuscript

52. Eddington DT, Puccinelli JP, Beebe DJ. Thermal aging and reduced hydrophobic recovery of polydimethylsiloxane. Sens Actuators, B Chem. 2006;114:170–2.

53. Kim J, Chaudhury MK, Owen MJ, Orbeck T. The mechanisms of hydrophobic recovery of polydimethylsiloxane elastomers exposed to partial electrical discharges. J Colloid Interface Sci. 2001;244:200–7.

54. Chen IJ, Lindner E. The stability of radio-frequency plasma-treated polydimethylsiloxane surfaces. Langmuir. 2007;23:3118–22. [PubMed: 17279784]

55. Hashimoto M, Shevkoplyas SS, Zasońska B, Szymborski T, Garstecki P, Whitesides GM. Formation of bubbles and droplets in parallel, coupled flow-focusing geometries. Small. 2008;4:1795–805. [PubMed: 18819139]

56. Roth J, Albrecht V, Nitschke M, Bellmann C, Simons F, Zschoche S, et al. Surface functionalization of silicone rubber for permanent adhesion improvement. Langmuir. 2008;24:12603–11. [PubMed: 18828614]

57. Matějíček J, Vilémová M, Mušálek R, Sachr P, Horník J. The influence of interface characteristics on the adhesion/cohesion of plasma sprayed tungsten coatings. Coatings. 2013;3:108–25.

58. Fu J,Chuah YJ,Ang WT,Zheng N,Wang D-A, Optimization of a polydopamine (PD)-based coating method and polydimethylsiloxane (PDMS) substrates for improved mouse embryonic stem cell (ESC) pluripotency maintenance and cardiac differentiation. Biomater Sci. 2017;5:1156–73. http://xlink.rsc.org/?DOI=C7BM00266A. [PubMed: 28509913]

59. Rim NG, Kim SJ, Shin YM, Jun I, Lim DW, Park JH, et al. Mussel-inspired surface modification of poly(L-lactide) electro-spun fibers for modulation of osteogenic differentiation of human mesenchymal stem cells. Colloids Surf B-Biointerfaces. 2012;91:189–97. [PubMed: 22118890]

60. Gomathi N,Mishra I,Varma S,Neogi S., Surface modification of poly(dimethylsiloxane) through oxygen and nitrogen plasma treatment to improve its characteristics towards biomedical applications. Surf Topogr Metrol Prop. 2015;035005:1–14.

61. Ding YH, Floren M, Tan W. Mussel-inspired polydopamine for bio-surface functionalization. Biosurf Biotribol. 2016;2:121–36. [PubMed: 29888337]

62. Lee H, Dellatore SM, Miller WM, Messersmith PB. Mussel-inspired surface chemistry for multifunctional coatings. Science. 2007;318:426–30. [PubMed: 17947576]

63. Hong S, Kim KY, Wook HJ, Park SY, Lee KD, Lee DY, et al. Attenuation of the in vivo toxicity of biomaterials by polydopamine surface modification. Nanomedicine. 2011;6:793–801. [PubMed: 21793672]

64. Jiang X, Christopherson GT, Mao H-Q. The effect of nanofibre surface amine density and conjugate structure on the adhesion and proliferation of human haematopoietic progenitor cells. Interface Focus. 2011;1:725–33. [PubMed: 23050077]

65. Lee JH, Jung HW, Kang I-K, Lee HB. Cell behaviour on polymer surfaces with different functional groups. Biomaterials. 1994;15:705–11. [PubMed: 7948593]

66. Shin YM, Lee YB, Kim SJ, Kang JK, Park JC, Jang W, et al. Mussel-inspired immobilization of vascular endothelial growth factor (VEGF) for enhanced endothelialization of vascular grafts. Biomacromolecules. 2012;13:2020–8. [PubMed: 22617001]

Author Manuscript Author Manuscript Author Manuscript Author Manuscript

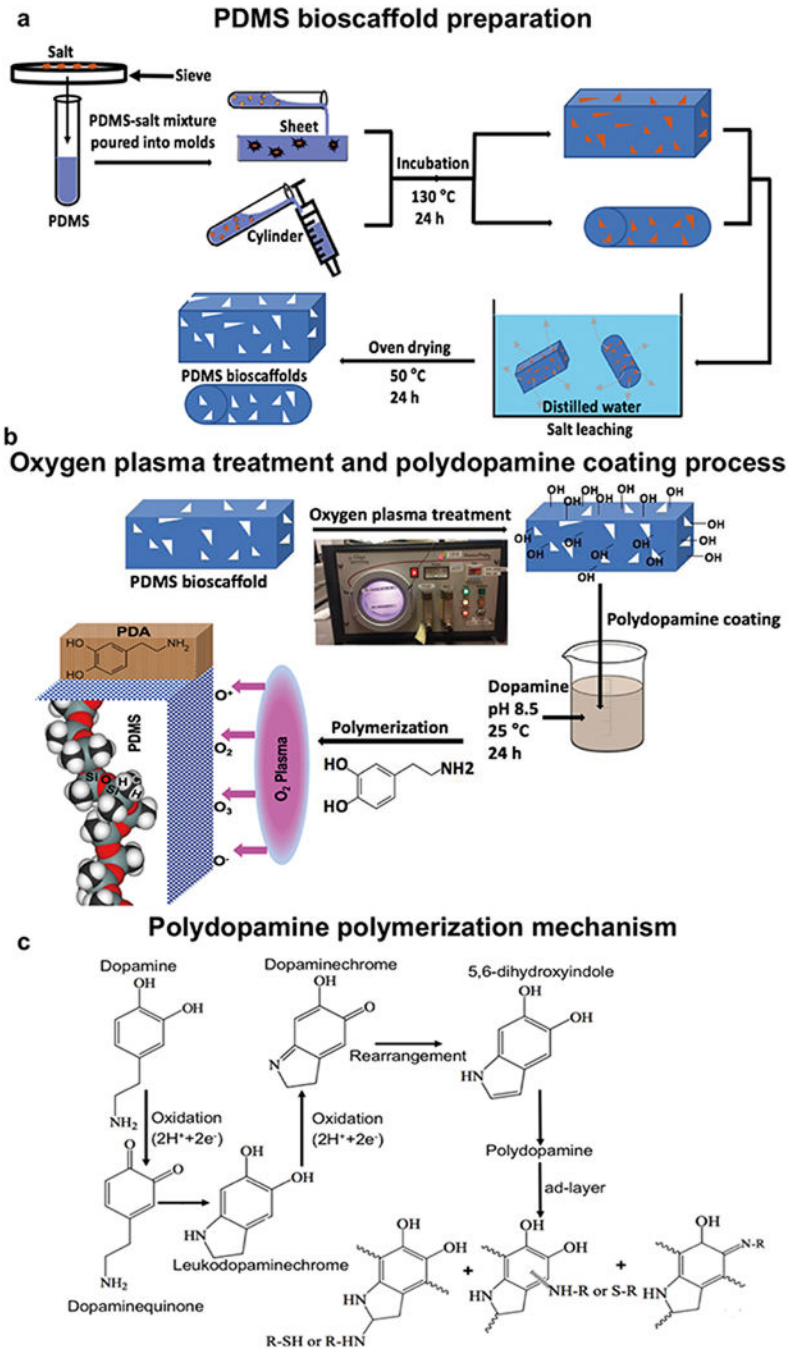

Fig. 1.

Schematic illustrations of the preparation of uncoated-, oxygen plasma treated- and polydopamine coated-PDMS bioscaffolds: **a** PDMS bioscaffolds were prepared using a SCPL technique with PDMS as the solvent and salt crystals as the particulate: salt was sifted through the sieves in order to obtain particles with a diameter of 275–350 μm. The salt particles were then mixed with a PDMS solution which was then poured and compressed on a microscopic glass slide for bioscaffold fabrication, followed by heat-curing at 130 °C for 24 h to permit cross-linking of the PDMS. The salt was finally leached by immersing the

Author Manuscript Author Manuscript Author Manuscript Author Manuscript

bioscaffold in deionized water for 72 h on a shaker with rotational speed of 200 rpm at 37 °C, with exchange of water two times a day. **b** The surface of PDMS bioscaffolds was modified by oxygen plasma treatment for 3 min at oxygen pressure of 0.3 mbar. Polydopamine was then coated by immersion of bioscaffolds into a dopamine solution (2 mg/ml in 10 mM Tris, pH 8.5) on a tube rotisserie. **c** Schematic illustration of the polydopamine formation mechanism which involves the oxidation of catechol in dopamine to quinone by alkaline pH-induced oxidation

Author Manuscript Author Manuscript Author Manuscript Author Manuscript

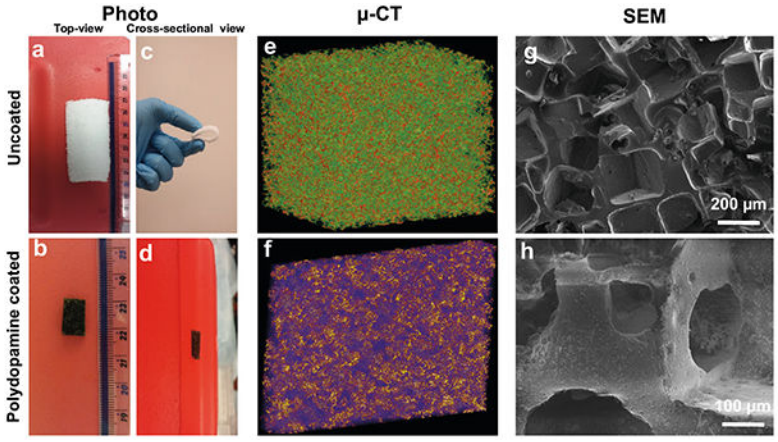

Fig. 2.

Photographs of the top-view (**a,b**) and cross-sectional view (**c,d**) of uncoated- (**a,c**) and polydopamine coated-(**b,d**) PDMS bioscaffolds showing the macrostructure and the color change from white to brown with polydopamine coating. The reconstructed μ-CT (**e,f**) and SEM images (**g,h**) of uncoated-(**a,c,e,g**) and polydopamine coated- (**b,d,f,h**) PDMS bioscaffolds

Author Manuscript Author Manuscript Author Manuscript Author Manuscript

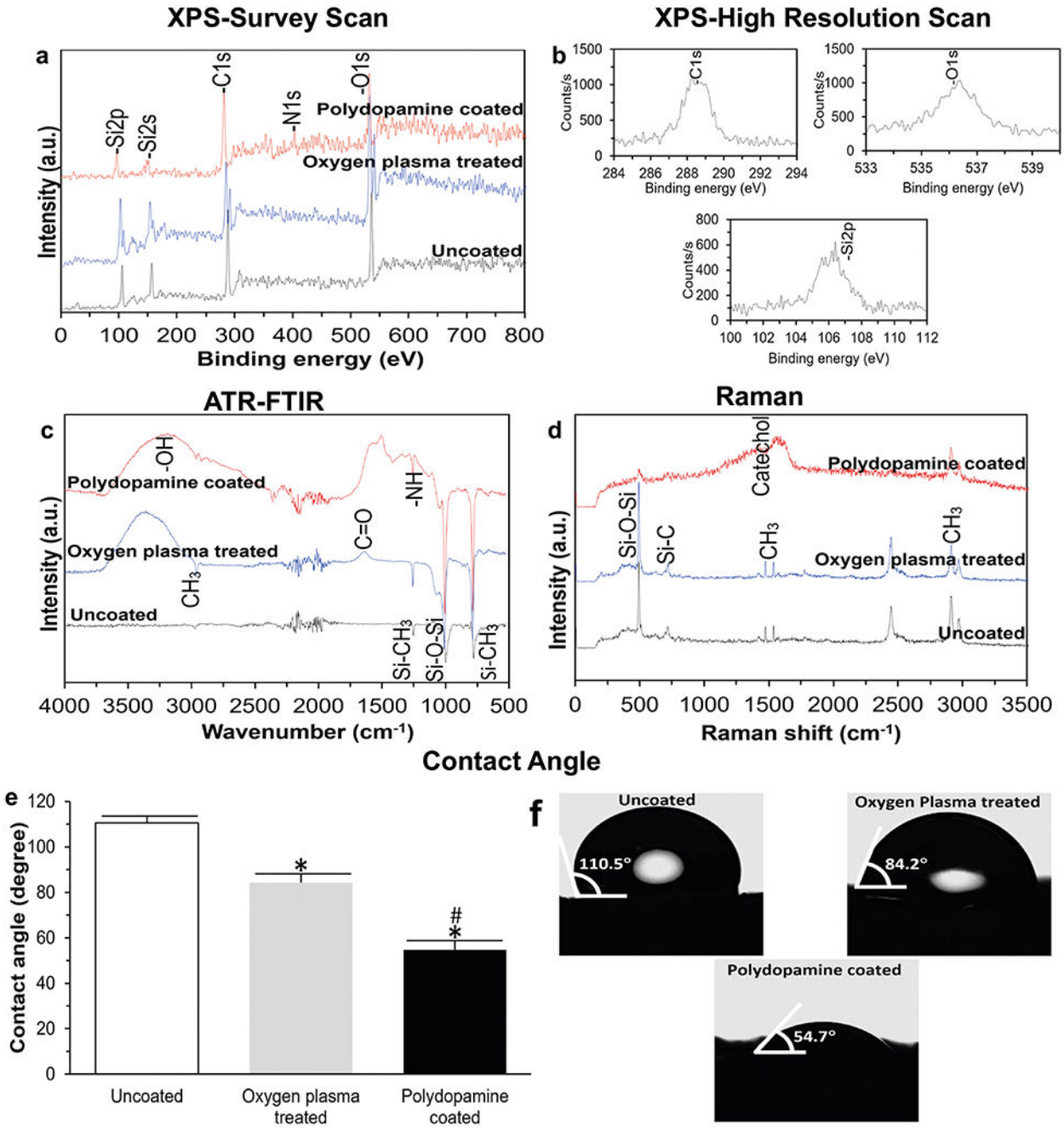

Fig. 3.

Survey (**a**) and high-resolution (**b**) scan XPS spectra showing qualitative XPS spectra of uncoated- and polydopamine coated-PDMS bioscaffolds. The survey spectrum and high-resolution spectra shows four elements of Si, C, N and O corresponding to the molecular formula of PDMS and polydopamine; **c** ATR-FTIR spectra validating the functional group transformation after the oxygen plasma treatment and polydopamine coating processes which was noticeable with the presence of C = O, –OH and N−H vibrations; **d** Raman spectra showing the intense stretching vibrations of the methyl group, Si–CH_3 and Si–O–Si corresponding to the PDMS and vibrations of catechol moieties in the polydopamine

Author Manuscript Author Manuscript Author Manuscript Author Manuscript

coating; **e,f** Water contact angle analysis showing the oxygen plasma treatment and polydopamine coating significantly decreased the hydrophobicity of uncoated-PDMS bioscaffold ($P < 0.05$). Significant differences: *$P = 0.000005$, difference between uncoated- and oxygen plasma treated- or polydopamine coated-PDMS bioscaffolds. $^{\#}P = 0.0008$, difference between oxygen plasma treated- and polydopamine coated-PDMS bioscaffolds. (Oneway ANOVA post hoc Tukey Test)

Author Manuscript
Author Manuscript
Author Manuscript
Author Manuscript

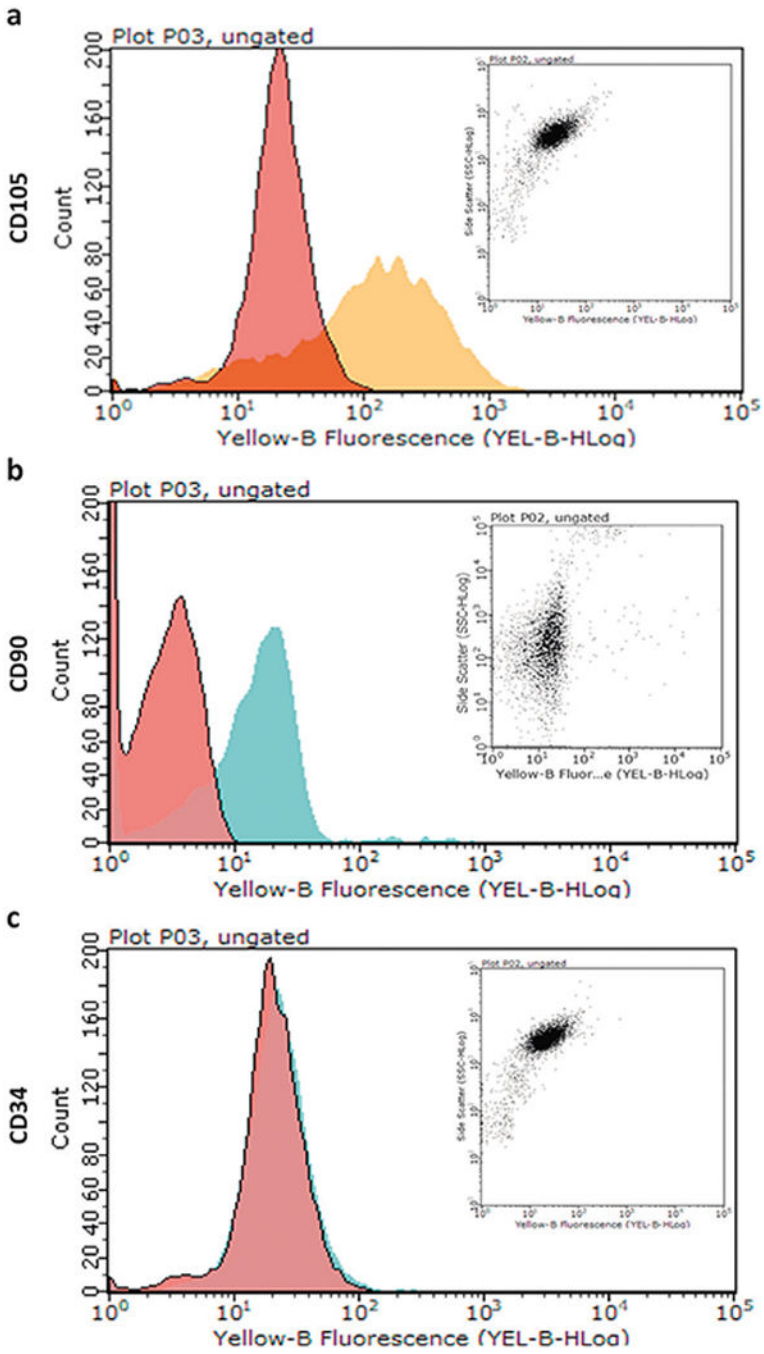

Fig. 4.

Cell surface expression of various AD-MSCs markers were detected by staining with specific monoclonal antibodies and analyzed by flow cytometry. AD-MSCs are CD105 **a** and CD90 **b** positive and CD34 **c** negative

Author Manuscript Author Manuscript Author Manuscript Author Manuscript

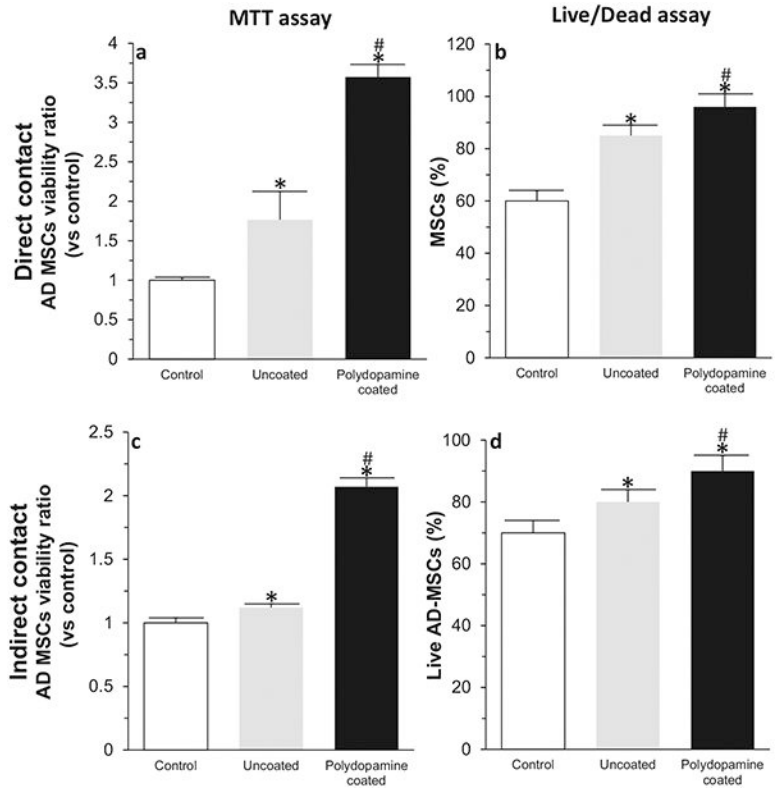

Fig. 5.

MTT **a,c** and Live/Dead **b,d** assays from both direct **a,b** and indirect **c,d** cell culture methods at day 10. Significant differences: MTT assay (direct contact): *P = 0.0004, difference between control group and uncoated- or polydopamine coated-PDMS bioscaffolds. #P= 0.002, difference between uncoated- and polydopamine coated-PDMS bioscaffolds. MTT assay (indirect contact): *P = 0.0000004, difference between control group and uncoated- or polydopamine coated-PDMS bioscaffolds. #P = 0.00003, difference between uncoated- and polydopamine coated-PDMS bioscaffolds. Live/Dead assay (direct contact): *P = 0.0001, difference between control group and uncoated- or polydopamine coated-PDMS bioscaffolds. #P = 0.04, difference between uncoated- and polydopamine coated-PDMS bioscaffolds. Live/Dead assay (indirect contact): *P = 0.0002, difference between control group and uncoated- or polydopamine coated-PDMS bioscaffolds. #P = 0.03, difference between uncoated- and polydopamine coated-PDMS bioscaffolds. (One-way ANOVA post hoc Tukey Test)

Author Manuscript Author Manuscript Author Manuscript Author Manuscript

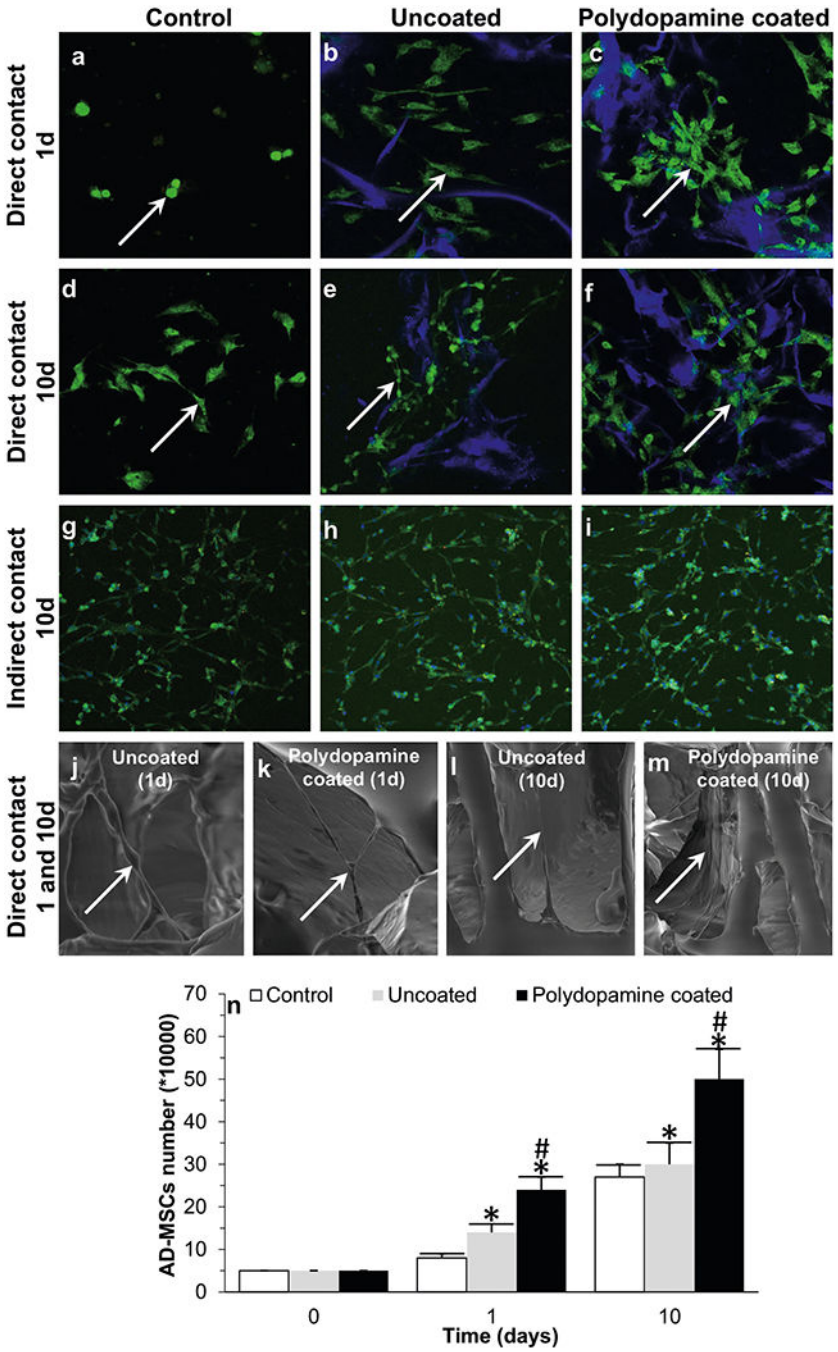

Fig. 6.

Confocal images of ADMSCs after 1 (**a–c**) and 10 (**d–i**) days seeding into uncoated- (**b, e**) and polydopamine coated- (**c, f**) PDMS bioscaffolds (direct contact: **a–f**) and culturing with the extracts of uncoated **h** and polydopamine coated- **i** PDMS bioscaffolds (indirect contact: **g– i**); SEM images of AD-MSCs (indicated by the white arrows) within the center of the uncoated (**j,l**) and polydopamine coated (**k,m**) PDMS bioscaffolds at day 1 (**j,k**) and 10 (**l,m**); and the results of AD-MSCs counting at day 0, 1 and 10 **n**. Significant differences: Day 1: *P = 0.0003, difference between control group and uncoated- or polydopamine

Author Manuscript Author Manuscript Author Manuscript Author Manuscript

coated-PDMS bioscaffolds. #P = 0.009, difference between uncoatedand polydopamine coated-PDMS bioscaffolds. Day 10: *P = 0.003, difference between control group and uncoated- or polydopamine coated-PDMS bioscaffolds. #P = 0.01, difference between uncoatedand polydopamine coated-PDMS bioscaffolds. (One-way ANOVA post hoc Tukey Test)